

CdS:In THIN FILMS GROWN BY CHEMICAL BATH

M. BECERRIL-SILVA^a, O. PORTILLO-MORENO^b, R. LOZADA-MORALES^b,
J. L. FERNANDEZ-MUÑOZ^{c*}, O. ZELAYA-ÁNGEL^a

^a*Departamento de Física, Centro de Investigación y de Estudios Avanzados del IPN. P.O. Box 14-740, México 07360 D. F.*

^b*FCFM, Posgrado en Optoelectrónica, Facultad de Ciencias Químicas, Benemérita Universidad Autónoma de Puebla, Puebla, México.*

^c*Centro de Investigación en Ciencia Aplicada y Tecnología Avanzada Unidad Legaria del Instituto Politécnico Nacional Legaria 694, Col. Irrigación, México D. F., México, C. P. 11500, México.*

By using the chemical bath deposition (CBD) technique, polycrystalline CdS thin films were prepared on glass and doped with In during the growth process by adding relative-volumes (V_R) of $\text{In}(\text{NO}_3)_3$ into the growing aqueous solution. No post-growth annealing on the layers was applied. In general, for the values of V_R used here, the lower (higher) V_R more (minor) efficient the In-doping mechanism. Furthermore, high V_R values induce the formation of In_2S_3 into CdS films. By means of thermoelectric power measurements the sign and density of carriers were determined, and it was found that majority carriers are electrons. For samples with low V_R values, the doping increases if V_R also increases. Dark conductivity (σ) measurements at room temperature indicate values of σ up to 3.5 orders of magnitude higher than undoped CdS. For samples grown with high V_R values, the optical absorption spectra clearly show two transitions one of them located on ~ 2.4 eV belonging to the fundamental energy gap (E_g) of CdS and the other one on ~ 2.1 eV, which has been associated to the E_g of In_2S_3 .

(Received April 4, 2016; Accepted January 26, 2017)

Keywords: Semiconductors; Chemical synthesis; Impurities in semiconductors; Electronic transport

1. Introduction

The research of the optical and electrical properties of semiconducting CdS layers has always been constant matter of attention for many researchers because of their applications [1-3]. CdS is an important semiconductor useful for photovoltaic [4], sensor [5], optical [6], among others, devices fabrication. In this work the increase of the density of carriers to improve the electrical conductivity (σ) with no change in the optical band gap (E_g) properties, was our main goal. Wide-band-gap window (2.4 eV) and a higher electrical conductivity can be obtained simultaneously by employing adequate growth methods. In our case, the chemical bath deposition (CBD) growth process was used to deposit and to dope CdS thin films at the same time. No annealing processes on the layers were added. In the past some works were reported about In-doping CdS by using other growth methods and even the CBD technique [7,8], however the doping process was not so efficient. In our case, the doping was effective and homogeneous because of the In-ions are substitutionally introduced inside the film during growth-process and no gradients in the In distribution are produced. Gradients in density of carriers arise in methods like ionic implantation.

*Corresponding author: jlfernandez@ipn.mx

2. Experimental details

The growth of polycrystalline CdS films was performed at 80 ± 1 °C on glass substrates. Details of the growth process have been previously reported elsewhere [9]. Salts reagents (concentrations) used in the CdS:In preparation were: CdCl₂ (0.02 M), KOH (0.15 M), NH₄NO₃ (1.5 M), SC(NH₂)₂ (0.2 M) and In(NO₃)₃·3H₂O (0.1 M). The total solution (100 ml) for growing CdS was completed with relative volumes (V_R) of the In(NO₃)₃ agent-solution from 1.0% until 10.0% in steps of 1% (1.0 ml). This allowed the study with ten different doping levels. Sample labeled CdS:In₀ corresponds to the undoped layer, and those labeled CdS:In₁-CdS:In₁₀ are the other doped ten samples, respectively. The thickness of layers, measured by utilizing a Dektak II profilometer, were in the range of 200 ± 10 nm. Average diameter of grains were 30 ± 10 nm. The structural characterization was carried out by means of the X-ray diffraction (XRD) data registered in a Siemens D-5000 diffractometer and employing the CuK_α line. Optical Absorption spectra allowed us to calculate the band gap energy (E_g) by using the α^2 versus $h\nu$ plot; here α is the optical absorption coefficient and $h\nu$ the photon energy. Dark conductivity measurements were achieved in vacuum in the absolute temperature range 100-450°K. The sign and concentration of carriers (n) were determined by means of thermoelectric power data.

3. Results and discussion

Spectra of doped and undoped CdS show the cubic zincblende (ZB) crystalline structure. In Fig. 1 the diffractograms of all the samples studied are exhibited. It can be observed how the CdS thin films grow mainly on the (111) direction. For CdS:In₁-CdS:In₄ samples the (111) interplanar distance was, in average, smaller than the one corresponding to the undoped sample. This reduction only can be a consequence of the incorporation of In into the lattice. The smaller ionic radius of In³⁺ (0.81 Å) as compared with that of Cd²⁺ (0.95 Å) can be the cause for the decreasing of the (111) interplanar distance. Of course, this occurs if In-ions enter substitutionally in Cd sites such as occur in some other cation-doping-CdS cases. In CdS:In₅ and CdS:In₆ the (111) interplanar distance (d_{111}) is larger than d_{111} of the CdS:In₀ sample, and we suppose in this case In enters in both substitutionally and interstitially manners. For CdS:In₇-CdS:In₁₀, In₂S₃ is formed on account of higher impurity concentration and also due to the electronic affinity between In³⁺ and S²⁻ that almost has the same value than the electronic affinity between Cd²⁺ and S²⁻ [10,11]. In Fig. 2, magnified XRD patterns of CdS:In₇ to CdS:In₉ are illustrated, in all these patterns a peak at $2\theta \cong 55.22^\circ$ and a faint signal at $2\theta \cong 52.3^\circ$ appear, which correspond to [200] and [112] planes of the hexagonal phase of In₂S₃ (γ -In₂S₃) [12]. The γ -phase of In₂S₃, considered as the high temperature modification in single crystals [13], has been observed in In₂S₃/ITO/glass films deposited by CBD [14]. In diffractograms of CdS:In₁ to CdS:In₆ samples the peaks of γ -In₂S₃ do not appear. The separation of In₂S₃ from CdS happens because the solubility of In₂S₃ in CdS has been observed to occur only until 2% [15].

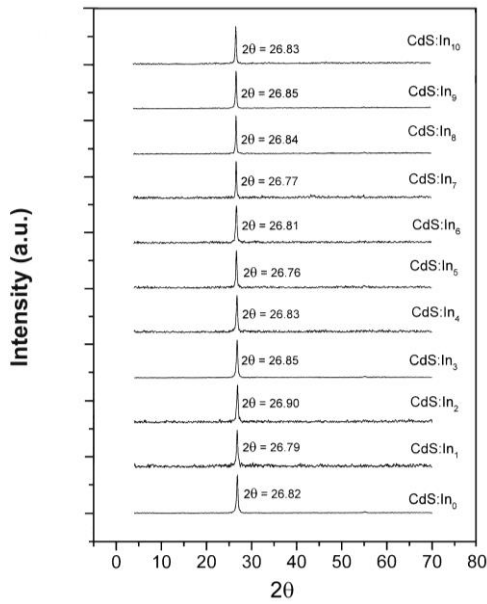


Fig. 1. Diffractograms of all the CdS:In layers studied. The solitary peak observed correspond to the [111] family of planes of the cubic phase.

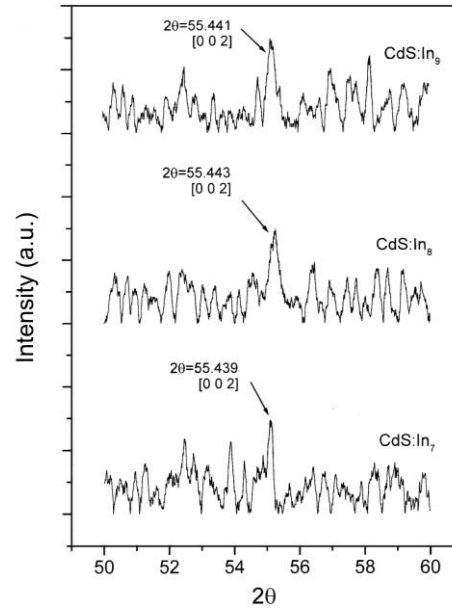


Fig. 2. XRD peaks corresponding to [002] and [112] planes of the hexagonal phase of In_2S_3 at $2\theta \cong 55.4^\circ$ and 52.3° , respectively, in samples CdS:In₇ – CdS:In₉.

The dark conductivity (σ) versus $1/kT$ plot is illustrated in Fig. 3, where k is the Boltzmann constant and T the absolute temperature. Measurements were carried out in the range $100 \leq T \leq 450$ K. For the samples CdS:In₁- CdS:In₆, σ increases so rapidly with respect to σ of CdS:In₀. All these doped samples exhibit a similar behavior and reach a relative maximum value of σ ($0.07 \Omega^{-1}\text{cm}^{-1}$) at $1/kT = 38.6$ (eV^{-1}), i.e., at room temperature (RT, $T= 300$ K). This property makes the layers very suitable to be used in electronic devices operating at this temperature. The difference between the higher σ values of CdS:In₄ and σ of CdS:In₀ at RT is ~ 3.5 orders of magnitude. Afterward, by using the Arrhenius method in the interval $38.6 \leq 1/kT \leq 47.0$ eV ($247 \leq T \leq 300$ K), where the mechanism predominant on σ is the thermoionic emission, the calculated average (including CdS:In₀) activation energy (E_A) was 0.26 ± 0.01 eV. A level with this E_A -value has been often found in undoped CdS having low or high values of resistivity [16-18]. In a previous work [19], we identified the depression observed in the curves at $T \sim 410$ K ($1/kT \sim 30$ eV^{-1}). We assumed it is originated by the annihilation of vacancy–interstitial ($V_{\text{Cd}}\text{-}I_{\text{Cd}}$) pairs of Cd, when Cd ions return to their original position. $V_{\text{Cd}}\text{-}I_{\text{Cd}}$ pairs appears when the metastable cubic zincblende (ZB) structure attempts to transform to the stable hexagonal wurtzite (W) structure when T rises, but the process is inhibited by the absence of sulfur vapor in the annealing-furnace, in which vacuum was done. These $V_{\text{Cd}}\text{-}I_{\text{Cd}}$ pairs are responsible of the bowing of the σ versus $1/kT$ curves before the maximum [19].

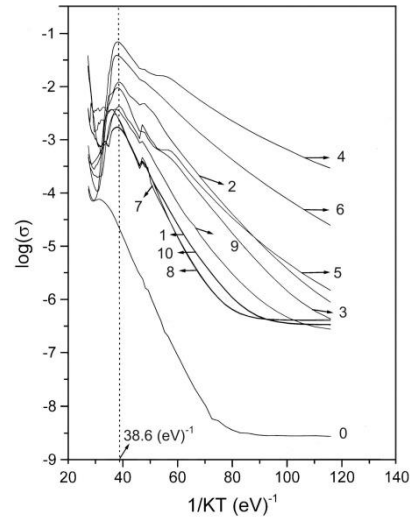


Fig. 3. $\text{Log}_{10}(\sigma)$ versus $1/kT$ in the range 100 – 450 K for all the samples studied.

Fig. 4 shows the $\text{log}(\sigma)$ vs $(KT)^{-1/4}$ plot for CdS:In₂, CdS:In₄, CdS:In₆, three representative doped samples. The straight line means that Mott's variable range hopping (VRH) mechanism dominates the transport of electrons at low temperatures, $0.26 \leq T^{-1/4} \leq 0.32$ ($95 \leq T \leq 218$ K). Ramaiah and coworkers [20] have observed this type of behavior in CdS:In films prepared by spray pyrolysis. The VRH functional dependence has been explained in Ref. 20 by demonstrating that for small CdS grain size, which is the case, the average grain size (l) of the polycrystalline CdS is shorter than the Debye length (L_D), since if $l \ll L_D$ grains are depleted and VRH occurs. In our case, since the size of grains is relatively larger, we think the $\text{log}(\sigma) \propto T^{-1/4}$ behavior is originated by the doping when great deal of In-atoms are included into the CdS microcrystals. Indium located in Cd²⁺ sites and in interstitial positions added to others structural defects like stacking faults, In-antisites and dislocations, give place to a great density of defects close to the Fermi level. At low T values the probability of electrons traveling through these defects is higher than the probability they move via extended states. For the rest of samples (CdS:In07 – CdS:In10) σ decays and the line-way changes as it can be seen in Fig. 3. In these samples σ does not follow the Mott's VRH mechanism at low temperatures; and the maximum of σ is also localized at ~ 300 K.

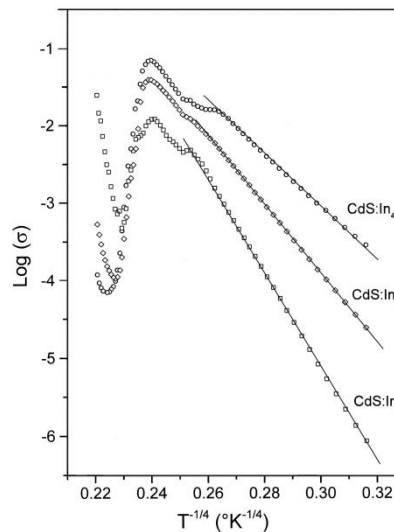


Fig. 4. $\text{Log}_{10}(\sigma)$ versus $T^{-1/4}$, characteristic of the variable range hopping conduction, for three CdS:In representative films.

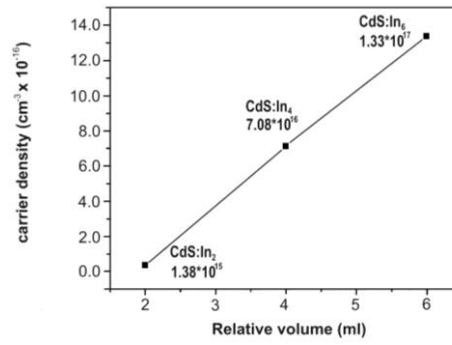


Fig. 5. Carrier density as a function of the relative volume (V_R) of $In(NO_3)$ added to the growing solution.

By means of thermoelectric power measurements at RT the density of carriers (n) was determined for the samples that do not follow the VRH conduction at low temperatures. In Fig. 5 is displayed how when V_R augments n also increases, this result is in agreement with our initial supposition that at RT In enters in Cd^{2+} sites as In^{3+} using two electrons to be bonded with S^{2-} , which allows it to transfer the additional electron to the CdS conduction band. Furthermore, from σ and n values at RT the mobility (μ) of electrons for CdS:In₂-CdS:In₆ was calculated. Fig. 6 evidences how μ diminishes when V_R increases. This could happen because if the density of In impurities increases, n increases, but on his part affect the periodicity of the lattice, then the electronic transport has less fluidity. Similar values of mobility have been reported for CdS:In polycrystalline films [23].

Table I. Energy band gap values data for samples CdS:In₇–CdS:In₁₀. E_{g1} for CdS and E_{g2} for In_2S_3 .

Sample	E_{g1} (eV)	E_{g2} (eV)
CdS:In ₇	2.39	2.14
CdS:In ₈	2.41	2.18
CdS:In ₉	2.44	2.27
CdS:In ₁₀	2.43	2.25

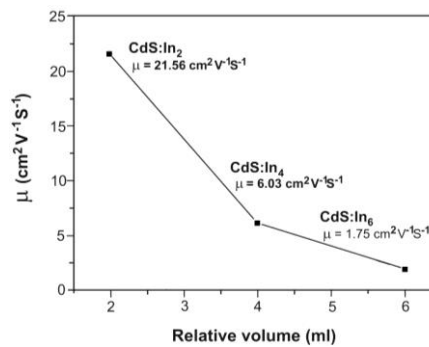


Fig. 6. Mobility (μ) as a function of the relative volume (V_R) of $In(NO_3)$ added to the growing solution.

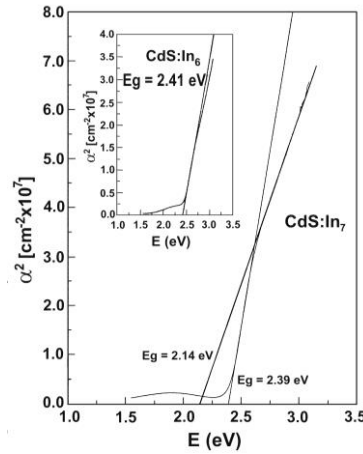


Fig. 7. α^2 versus the photon energy ($h\nu$) plot for the CdS:In₇ film. The inset displays the same plot for the sample CdS:In₆. The intercept of the straight line with the energy axis determines the value of E_g .

In the optical absorption measurements, the E_g value was calculated by using the well known relation $\alpha^2 = cte(E_g - h\nu)^{1/2}$ [21]. The E_g value found for cubic CdS:In₀ was 2.42 eV, as already reported [22]. For the rest of samples the absorption spectra were grouped in two parts: group I, CdS:In₁ - CdS:In₆, and group II, CdS:In₇ - CdS:In₁₀. The spectra of CdS:In₇ and CdS:In₆ are shown in Fig. 7 and in its inset, respectively. In the spectrum of CdS:In₆ one can observe only a small deviation, owing to the In³⁺ incorporated as an impurity, at high energies, of the expected line-way of the fundamental edge. The E_g value is slightly modified as it occurs with all the samples of group I. In the spectrum of CdS:In₇, two transitions are observed. The same fact occurs in all the samples of group II. The data values of these transitions are showed in the Table I. The first transition is associated with the fundamental band gap of CdS ($E_{g1} = 2.42 \pm 0.05$ eV) and the second one is assigned to absorption edge of In₂S₃ ($E_{g2} = 2.20 \pm 0.07$ eV). E_g of In₂S₃ varies between 2.0 and 2.05 depending on the growth method [15,23], although for γ -In₂S₃ an E_g of 2.75 eV has been reported [14].

4. Conclusions

In summary, CdS thin films have been In-doped during the growth process and no annealing was made for this study. In samples CdS:In₁-CdS:In₆, grown with relative low concentrations of In(NO₃)₃, doping was carried out more efficiently than on the CdS:In₇-CdS:In₁₀ films, grown with high In(NO₃)₃ concentration.

In the first group dark conductivity increased up to 3.5 orders of magnitude for CdS:In₄ with respect to undoped layers, and their E_g values have in practice the same values of undoped CdS. Samples of the second group had lower σ values and two E_g values were found in each film, one corresponding to CdS and another one associated to the arising of In₂S₃ microcrystals.

Acknowledgements

Authors thank to Z. Rivera and M. Becerril for their technical assistance. This work was partially supported by CONACyT-México.

References

- [1] J Schroeder, PD. Persans J Lumines; **70**, 69 (1996)
- [2] C. Klingshim Phys Stat Solidi B; **202**, 857 (1997)
- [3] AM. Hermann Sol En Mater Sol Cells **55**, 75 (1998).
- [4] CS Ferekides, D Marinskiy, V Viswanathan, B Tetaly, V Palekis, P Selvaraj, DL Morel . Thin Solid Films; **361/362**, 520 (2000).
- [5] BK Maremadi, K Colbow, Y. Harima Rev Sci Instrum; **68**, 3898 (1997).
- [6] M Kobayashi, K Kitamura, H Umeya, AW Jia, A Yoshikawa, M Shimotomai, Y Kato, K. Takahashi J Vac Sci Technol B **18**, 1684 (2000).
- [7] U Neukirch, I Broser, R. Rass Semicond Sci Technol; **6**, A96 (1991)
- [8] RS Mane, CD. Lokhande Mater Chem Phys **65**, 1 (2000).
- [9] JL Martínez, G Martínez, G Torres-Delgado, O Guzmán, P del Ángel, O Zelaya-Ángel, R. Lozada-Morales J Mater Sci Mater Electron **8**, 399 (1997)
- [10] EC. Baughan Faraday Trans **51**, 1863 (1961).
- [11] P. Politzer, Faraday Trans **64**, 2241 (1968)
- [12] JCPDS –ICDD X–Ray diffraction card number 33 – 0623.
- [13] R Diehl, R. Nitsche, J Crys Growth **28**, 306 (1975)
- [14] CD Lokhande, A Ennaoui, PS Patil, M Giersig, K Diesner, M Muller, M. Tributsch Thin Solid Films; **340**, 18 (1999).
- [15] VN Semenov, OV Ostapenko, AN Lukin, M. Averbakh Inorg Mater **36**, 160 (2000).
- [16] KH Nicholas, J. Woods Brit J Appl Phys **15**, 783 (1964)
- [17] AA Istratov, OF. Vyvenko Semicond; **29**, 340 (1995)
- [18] G Grill, G Bastide, G Sagnes, M. Rouzeyre J Appl Phys **50**, 1375 (1979).
- [19] R Lozada-Morales, M Rubín-Falfan, O Zelaya-Ángel, R Ramírez-Bon, J Phys Chem Solids **59**, 9 (1998).
- [20] KS. Ramaiah J Mater Sci Mater Elect; **10**, 291 (1999)
- [21] JL. Pankove *Optical Processes in Semiconductors*, Dover Pub., 1971, P. 36.
- [22] O Zelaya-Ángel, JJ Alvarado-Gil, R Lozada-Morales, H Vargas, F. da Silva, Appl Phys Lett; **64**, 291 (1994).
- [23] J Herrero, J. Ortega Sol Ener Mater **17**, 357 (1988).